

ICE GENESIS

Creating the next generation of 3D simulation means for icing

Type of action: Research and Innovation Action

Call identifier: H2020-MG-2018-SingleStage

Topic: MG-2-5-2018 Innovative technologies for improving aviation safety and certification in icing conditions

Deliverable D6.3

Assessment of improved FZDZ capabilities for each IWT involved in the project

EC Grant Agreement number:

824310

Start date of project: 1 January 2019

Duration: 60 months

Lead beneficiary of this deliverable:

CIRA

Due date of deliverable: 30/06/2021

Actual submission date: 28/03/2024

Version #: R0.2

Project funded by the European Commission within the H2020 Programme (2014-2020)		
Type		
R	Document, report excluding the periodic and final reports	X
DEM	Demonstrator, pilot, prototype	
DEC	Websites, patents filing, press & media actions, videos, etc.	
OTHER	Software, technical diagram, etc.	
ETHICS	Ethics requirement	
ORDP	Open Research Data Pilot	
Dissemination level		
PU	PUBLIC, fully open, no embargo e.g. web	X
PU+E1	PUBLIC after embargo of 12 months from date of publication	
PU+E3	PUBLIC after embargo of 3 years after the project's end	
RE	RESTRICTED, only for certain members of the consortium (including the Commission Services): all the consortium except Russian partners	
CO	CONFIDENTIAL, only for members of the consortium (including the Commission Services)	
CO+IGAB	CONFIDENTIAL, only for members of the consortium (including the Commission Services) and for the ICE GENESIS Advisory Board	

Revision History

V #	Date	Description / Reason of change	Author
0.1	01.03.2024	First Version	B. Esposito (CIRA)
0.2	12/03/2024	Update following reviewers' comments	B. Esposito (CIRA)

Deliverable Contributors

Authors

Organisation	Authors' name	Export control status date	Export control status
CIRA	Biagio Esposito	11/03/2024	No data subject to export control

Contributors

Organisation	Authors' name	Export control status date	Export control status
DLR	Romy Heller	11/03/2024	No data subject to export control

Export Control Status

Author / Contributor	Type of data	Position in document of concerned text/data*	Jurisdiction and ECCN under this jurisdiction	Status of authorization
CIRA,	Requirements and specifications, Scientific Papers, Computational data, Experimental data	§ 4, 5	No data subject to export control	Not Applicable
DLR	Experimental data	§5.3.2	No data subject to export control	Not Applicable

****To be checked by the Owner of the document before delivery of the document!***

Internal Reviewers

Organisation	Internal Reviewers' name
Airbus	Olivier Blesbois
Dassault	François Caminade

Table of Contents

1	Glossary.....	6
2	Executive Summary.....	7
3	Introduction	8
4	EASA CS-25 Appendix O – Freezing Drizzle requirements	9
4.1	Freezing Drizzle MVD < 40 µm (FZDZ-In)	9
4.2	Freezing Drizzle MVD > 40 µm (FZDZ-Out)	10
5	CIRA Icing Wind Tunnel.....	12
5.1	Feasibility Study	13
5.2	SBS Configurations and Rationale for the Matrix of Cloud Conditions.....	14
5.3	PSD/MVD Measurements and Preliminary Results for FZDZ Conditions	16
5.3.1	PSD/MVD Test Matrix	16
5.3.2	PSD/MVD Results from Preliminary SLD Calibration	18
5.4	LWC measurements.....	22
5.4.1	LWC uniformity	24
6	Conclusion.....	27
7	References	28

Table of Tables

Table 1: MVD, Dmax and LWC values for each SLD subset [7]	9
Table 2: Spray bar system configurations with the indication of the type and number of active spray nozzles in use during the PSD/MVD and LWC measurements at the center of the test section.....	15
Table 3: Matrix of cloud conditions (in the first column) used during the PSD/MVD cloud characterization with DLR CCP probe.	17

Table of Figures

Figure 1: Average cumulative mass spectrum compared to each individual cumulative mass spectra for FZDZ MVD < 40 μm (left) and FZDZ MVD > 40 μm (right) [8].....	10
Figure 2: Average cumulative mass spectrum compared to each individual cumulative mass spectra for FZDZ MVD < 40 μm (left) and FZDZ MVD > 40 μm (right) (Federal Aviation Administration FAA, 2009)	10
Figure 3: The 99% LWC envelopes vs temperature for FZDZ compared with 300-s data (left), altitude vs temperature envelopes for FZDZ compared to 30-s Data (right).....	11
Figure 4: CIRA Icing Wind Tunnel layout with main information on the test section configurations and performance.....	12
Figure 5: CIRA-IWT sketch showing the geometry considered for the CFD simulation with the test leg of the MTS configuration and the SBS.....	14
Figure 6: Study of the spray bar performance when equipped with two spray nozzle types. The first phase of this study analyses the main bi-phase flow parameters inside and outside each spray nozzle type. The simulation of the cloud inside the IWT test leg duct (phase 2) includes the assessment of LWC homogeneity with indication of potential PSD (normalized volume distribution) modifications due to different spray nozzle patterns on the spray bar module: (a) The two type of the spray nozzles are alternating on each bar; (b) each bar has a different spray nozzle (the even bars are those that produce large drops, and the odd bars are those that produce the smaller drops).	14
Figure 7: Water spray concentration measured by LSI system in the spray plume generated by single-jet (on the left) and multi-jet (on the right) spray nozzle.	16
Figure 8: DLR CCP (Cloud Combination Probe) on the left, installed in the centerline of the CIRA IWT test section during the PSD/MVD measurement slot. CIRA 4D-PDI on the right installed with sample volume located on the centerline, in the same position of DLR CCP.	18
Figure 9: Cumulative volume fraction measured for each test point (TP) by CCP and 4D-PDI at 110 ms^{-1} , with 1A2_SLD2 of SBS configuration.	18
Figure 10: Cumulative volume fraction measured by CCP probe at 110 ms^{-1} measured with 1A2_SLD3 of SBS configuration.	19
Figure 11: Cumulative volume fraction measured by CCP and PDI probe at 110 ms^{-1} measured with 1A3_SLD6 of SBS configuration.	19
Figure 12: Cumulative volume fraction measured by CCP and PDI probe at 110 ms^{-1} measured with 1A2_SLD5 of SBS configuration.	20
Figure 13: Example of the quantile-quantile plot showing the agreement between the measured PSD and Appendix O requirement with 1A2_SLD3 spray bar configuration. Data has been collected by CCP probe at 110 ms^{-1} and at pressure altitude of 6096 m.	20
Figure 14: Effect of the spray bar configurations on water mass distribution for the same condition: 110 ms^{-1} of airspeed with the SBS setting at the same air and water pressures (case a and c) excluding the case (b) with half spray nozzles setting at higher pressures to generate the smaller droplets.	21

<i>Figure 15: LWC measurements with RP installed on the strut to locate its sampling volume at the centerline of the CIRA-IWT test section. The plot on the top shows the sensor element temperature during the acquisition and between each test point. TWC behaviour for some conditions is shown in the bottom plot.</i>	22
<i>Figure 16: Cloud LWC calibration generated by 1A2_SLD2 spray bar configuration at 110 ms⁻¹ and with pressure altitude at sea level.</i>	23
<i>Figure 17: LWC calibration envelope for FZDZ cloud conditions generated by 1A2_SLD2 spray bar configuration.....</i>	23
<i>Figure 18: Cloud uniformity for one of the Appendix C conditions was measured with an Icing Grid at 60 ms⁻¹ at sea level of pressure altitude. Cloud has been generated with 1A2_SLD3 spray bar configuration at minimum MVD.</i>	24
<i>Figure 19: Variation of the ice thickness along the three cylinders located in the reference area of the test section. 1A2_SLD2 spray bar configuration has been used to generate 110 μm of MVD cloud with 0.5 gm⁻³ of LWC.....</i>	26

1 Glossary

Abbreviation / Acronym	Description/meaning
2D-C	Optical Array Probe
CCP	Cloud Combination Probe
CDP	Cloud Droplet Probe
CIP	Cloud Imaging Probe
FSSP	Forward Scattering Spectrometer Probe
FZDZ	Freezing Drizzle
LSI	Laser Sheet Imaging
LWC	Liquid Water Content
MVD	Median Volumetric Diameter
MW	Multi-Wire probe
PMS	Particle Measuring Systems
PSD	Particle Size Distribution
RP	Robust Probe
RR	Rosin-Rammler distributions
SAT	Static Air Temperature
SBS	Spray Bar System
SLD	Supercooled Large Droplet
TWC	Total Water Content
ZLE	Freezing Drizzle

2 Executive Summary

The scope of this deliverable is to provide a summary of the improvements performed by facilities during the first part of the program to achieve the capability to generate SLD cloud conditions focused on the Freezing Drizzle (FZDZ) envelope in compliance with FAA 14 CFR Part 25 and EASA CS-25 Appendix O. At the beginning of the program, six wind tunnel owners were involved in the ICE-GENESIS Work Package 6 (SLD Test Capability), CIRA, MINDEF, RTA, TUBS, TSAGI, and CIAM. However, the partnership with TSAGI and CIAM was terminated for geopolitical reasons in 2022. Moreover, MINDEF also discontinued its activities in ICE-GENESIS due to an incompatibility between the program's activity plans and their own. Therefore, from the original target of improving all the European facilities for SLD capability, the CIRA-IWT was the only one accomplishing this task, considering the RTA Icing Wind Tunnel had completed its improvement with the spray bar upgrading capabilities to the SLD cloud before the beginning of the ICE-GENESIS program. Therefore, this report highlights the main steps accomplished by CIRA during the selection of new spray nozzles to use as retrofit of the one available in the Spray Bar System (SBS), aiming to reproduce the SLD cloud with features close to the requested SLD freezing drizzle conditions. The report underlines the importance of the simulation model to characterize the bi-phase flow, whether in the spray nozzles or the tunnel test leg, to identify better the spray nozzle layout on the SBS that may help provide qualitative information on main parameters achievable in the reference area of the test section such as the cloud uniformity, droplet temperature. Different SBS configurations have been partially characterized during the measurement phases of the calibration campaign to validate the strategy used to maintain a PSD close to the requirement with a range of low LWCs in compliance with the requirement. The results of this effort have been synthesized in this report.

3 Introduction

The goal of the ICE GENESIS project is to improve the experimental testing capabilities of icing facilities to reproduce representative Supercooled Large Droplet (SLD) cloud conditions to define a common calibration methodology. In this report, an introduction of the FAA 14 CFR Part 25 and EASA CS-25 Appendix O are summarised, followed by a description of the activities performed in the CIRA-IWT with the selection of the new spray nozzle with the preliminary performance achieved in the generation of the FZDZ conditions.

4 EASA CS-25 Appendix O – Freezing Drizzle requirements

In this section, the SLD icing conditions defined in Appendix O of the EASA Certification Specification CS-25 Amendment 23 [1] are summarized. In general, the SLD conditions can be segregated into four subsets which include conditions with maximum drop sizes below 500 μm and higher than 500 μm in diameter, each with median volumetric diameters (MVDs) below 40 μm and larger than 40 μm (Table 1).

Freezing drizzle (FZDZ) refers to icing environments with maximum diameters of less than 500 μm whereas environments with maximum diameters exceeding 500 μm are referred to as freezing rain (FZRA). Those two conditions are then further distinguished based on the MVD. “FZDZ In” and “FZRA In” refer to environments with MVDs of smaller than 40 μm (mainly occurring within clouds). “FZDZ Out” and “FZRA Out” refer to environments with MVDs of larger than 40 μm (mainly occurring below clouds).

For each SLD subset, envelopes of maximum LWC values as a function of the horizontal extent and temperature are available. The particle size distributions (PSDs) and LWC envelopes are based on in-situ measurements performed between 1995 and 2000, which include the first and third Canadian Freezing Drizzle Experiment [2], [3], the First International Satellite Cloud Climatology Project Regional Experiment Arctic Cloud Experiment [4], the First Alliance Icing Research Study [5], as well as the SLD Flight Research Study by NASA Glenn [6]. The main instrumentation used during the field projects were PMS FSSP probes for the small droplet spectra and PMS 2D-C, 2D-G and 2D-P probes for the large particles. PMS King LWC probes and Nevzorov LWC-TWC probes were used for the water content measurement except for very low LWC, of which the values have been integrated from PSDs collected by optical spectrometers. In Table 1, an overview of the expected MVD range, maximum droplet diameter and maximum LWC for the different conditions is given [7].

Table 1: MVD, D_{max} and LWC values for each SLD subset [7]

Definition	MVD Range	D_{max} Range	MVD	D_{max}	LWC_{max}
FZDZ In	< 40 μm	100 – 500 μm	20 μm	389 μm	0.44 g/m^3
FZDZ Out	> 40 μm	100 – 500 μm	110 μm	474 μm	0.27 g/m^3
FZRA In	< 40 μm	> 500 μm	19 μm	1553 μm	0.31 g/m^3
FZRA Out	> 40 μm	> 500 μm	526 μm	2229 μm	0.26 g/m^3

4.1 Freezing Drizzle MVD < 40 μm (FZDZ-In)

The PSD requirements for FZDZ with an MVD smaller than 40 μm are shown in Figure 1. The average MVD is 20 μm and comes from the average of all of the cumulative mass spectrums (1469 points) with an average maximum diameter of 389 μm . Figure 2 shows the individual measured PSDs and the average cumulative mass spectrum (black line). Characteristic for this condition is the very low contribution of large particles (> 100 μm) to the overall mass, which is only about 10%. The 99.0% LWC of all of the cloud measurements was 0.44 g/m^3 , which is used as the upper limit at 0°C ambient temperature in Appendix O. The lower temperature limit for “FZDZ In” is -25°C with a maximum LWC of 0.29 g/m^3 . The maximum observed LWC during the flight campaigns was 0.77 g/m^3 [7]. Figure 3 shows the 99.0% LWC and altitude envelopes versus ambient temperature during the performed flight test campaigns. The numbers of data points observed for each subset of FZDZ data are shown in the caption. A different number of data points is available for PSD and LWC measurements. The term ZLE in the description refers to Freezing Drizzle.

4.2 Freezing Drizzle MVD > 40 μm (FZDZ-Out)

The PSD requirements for FZDZ with an MVD of larger than 40 μm are shown in Figure 1. The average MVD is 110 μm and comes from an average of all of the cumulative mass spectrums (335 points) with an average maximum diameter of 474 μm. Figure 2 shows the individual measured PSDs during the performed flight test campaigns and the average cumulative mass spectrum (black line). The 99.0% value of the LWC of all of the cloud measurements was 0.27 g/m³, which is used as the upper limit at 0°C ambient temperature in Appendix O. The lower temperature limit for “FZDZ Out” is also -25°C with a maximum LWC of 0.18 g/m³. The maximum LWC observed during the flight campaigns was 0.39 g/m³. [2]. Figure 3 shows the 99.0% LWC and altitude envelopes versus ambient temperature. The numbers of data points observed for each subset of FZDZ data are shown in the caption.

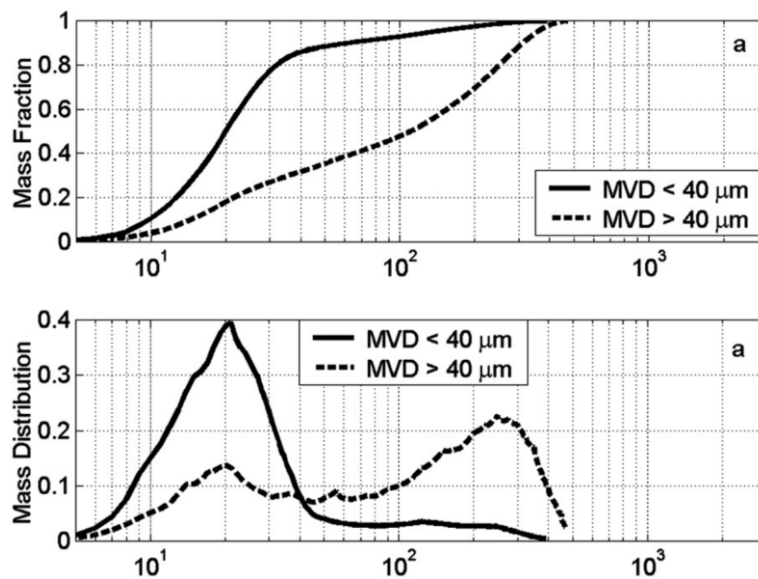


Figure 1: Average cumulative mass spectrum compared to each individual cumulative mass spectra for FZDZ MVD < 40 μm (left) and FZDZ MVD > 40 μm (right) [8]

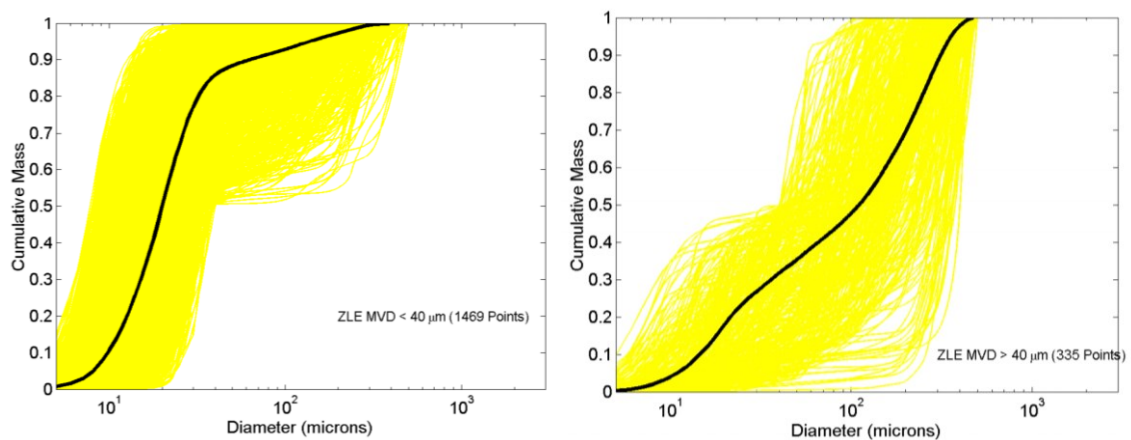


Figure 2: Average cumulative mass spectrum compared to each individual cumulative mass spectra for FZDZ MVD < 40 μm (left) and FZDZ MVD > 40 μm (right) (Federal Aviation Administration FAA, 2009)

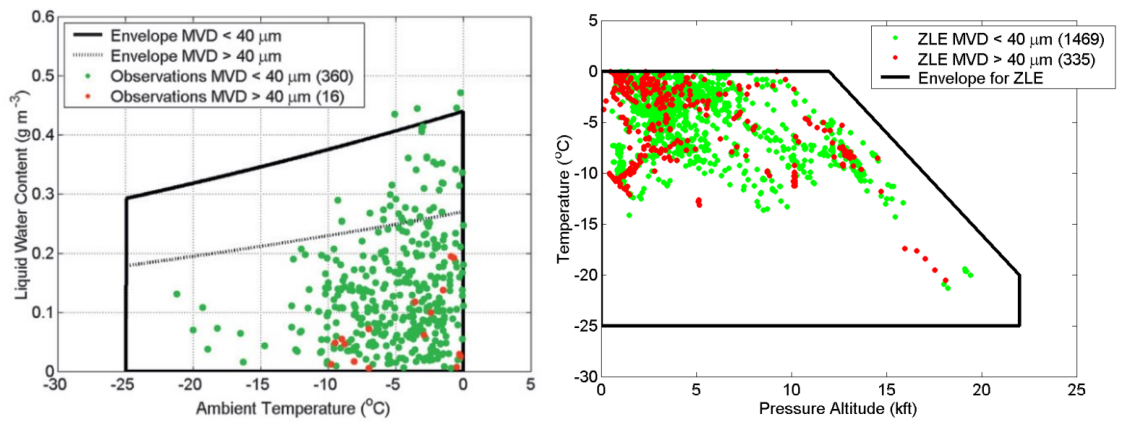


Figure 3: The 99% LWC envelopes vs temperature for FZDZ compared with 300-s data (left), altitude vs temperature envelopes for FZDZ compared to 30-s Data (right)

5 CIRA Icing Wind Tunnel

This facility has three interchangeable test sections and one open jet configuration. The aero-line with main internals and configurations is shown in *Figure 4* with a table summarizing main performances. Some features are still unusual for large icing wind tunnel: downstream the fan diffuser, a twin row heat exchanger is also capable to control the air Relative Humidity (RH) before the spray bar, by means of a hot air compressor and steam injection. Controlled humidity ranges between 70% and 100% for temperatures between -15°C and -20°C . 100% humidity value can be set between -20°C and -40°C . Control accuracy is within $\pm 5\%$ RH.

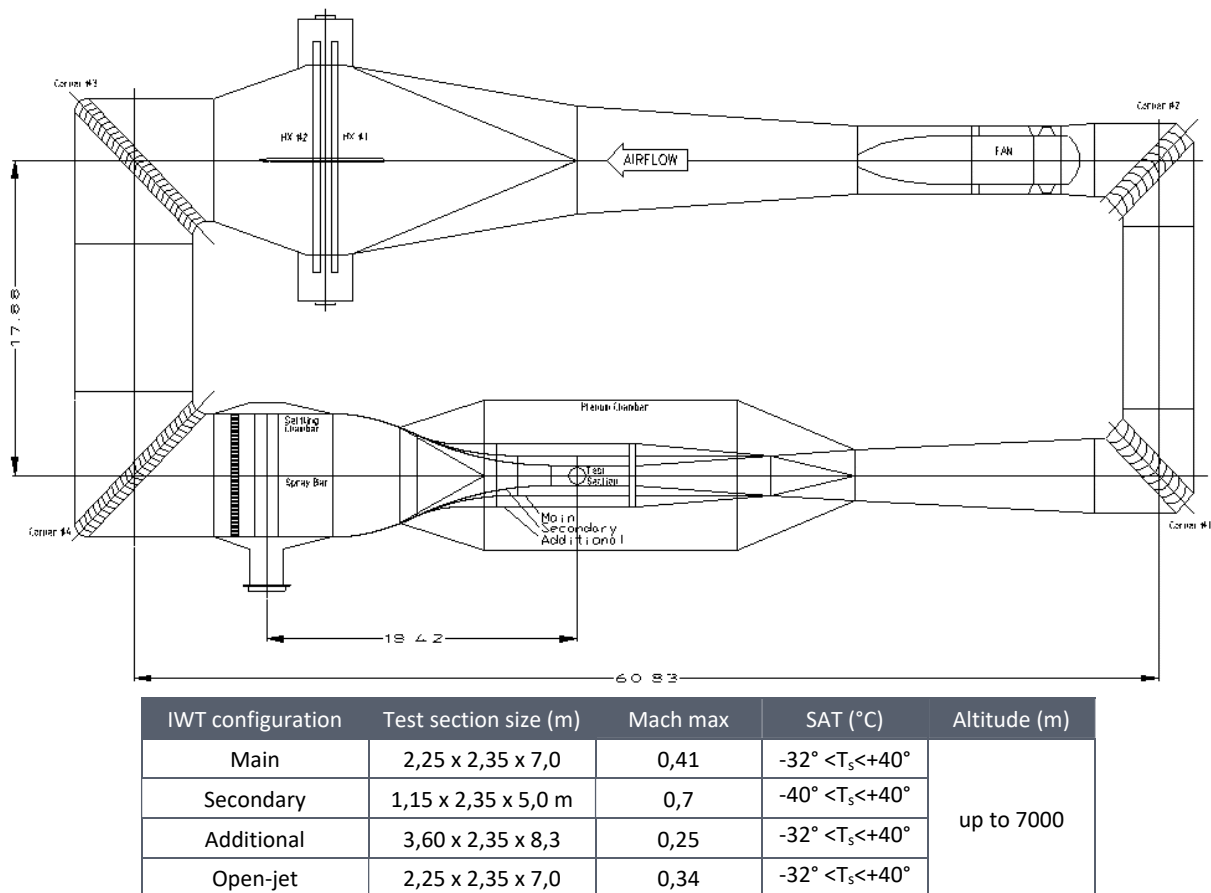


Figure 4: CIRA Icing Wind Tunnel layout with main information on the test section configurations and performance

The facility settling chamber is fitted with a honeycomb module to reduce large scale eddies thus ensuring flow straightening. Downstream the honeycomb, an interchangeable section provides the possibility to switch the spray bar module with the screens module to improve the flow quality in the test section allowing the execution of the aerodynamic tests. A 0.7 MW centrifugal compressor unit allows the pressure to be regulated between 0.39 bars (corresponding to an altitude of 7000 meters) and 1.45 bars. While depressurization is used to simulate altitude for icing tests, pressurization, combined with a reduction in air temperature, helps to increase the Reynolds number for aerodynamic tests.

The SBS is located in the IWT stilling chamber, about 18 meters upstream the centre of test section, thus assuring a droplet residence time higher enough to achieve super-cooling conditions even for large droplet sizes. The SBS has 20 bars having a low drag aerodynamic shaped section, whose main feature is a low sensitivity to flow separation. Each bar is removable and may be vertically adjusted for optimising cloud coverage and uniformity, if necessary, during the calibration phase. Two spray nozzle types, one for small droplet spray and another for large droplet spray at the same air and water

pressure settings, were selected to produce low LWCs to define an SLD envelope as close as possible to the Appendix O requirement for expected airspeed range. The two spray nozzle types were installed on each bar alternately until they covered its central section with up to 30 spray nozzles that can be remotely and independently activated through a solenoid valve using the same air and water manifolds for both. Thirty of twenty spray bars were used during the calibration, changing the number of operating spray nozzles on the base of condition (LWC and cloud uniformity) to reproduce by Facility Management System Software. Therefore, the SBS may use a single spray nozzle type (up to 15 per bar) to reproduce one PSD mode (small PSD-mode or large PSD-mode) or both spray nozzle types for bi-modal PSD clouds. The last SBS configuration can operate using the same air and water pressure settings for all the bars, taking advantage of different spray plume characteristics to generate bi-modal clouds. Another modality to operate using this configuration of the SBS is to set different air and water pressures to the odd bars with respect to the even bars. With this modality, water mass may change independently for each mode forming the PSD of the bimodal clouds.

5.1 Feasibility Study

Before to proceed with cloud calibration, to predict the behaviour of the SBS with different configurations, a simulation model was built considering the CIRA-IWT test-leg geometry (*Figure 5*). This model was based on Ansys-Fluent limited to the CIRA-IWT test leg with the spray bar configuration setting with two types of spray nozzles to generate bi-modal cloud condition at 110 ms^{-1} have been studied. A model with more than 12×10^6 of polyhedral cells has been developed to study the effect of modified spray bar parameters and spray nozzles layout on main cloud proprieties in the test section (e.g., droplets' trajectories, droplets' temperature, droplet diameters distributions).

Results have shown the possibility to predict potential overlap of water mass in the reference area of the test section due to large droplets trajectories which amplitude depends of the spray nozzle plume angle combined by location of the spray nozzle on the spray bar. The simulation of the internal flow profiles for both velocity and water volume fraction have been studied for each spray nozzle types to predict the spray plume angle for representative air/water pressures. Results have been combined with experimental characterization of each spray nozzle type for a series of air/water pressures that provide the droplet diameter statistics. The measurements have been used for building the PSDs based on the Rosin-Rammler (RR) distributions for CFD input. These distributions with information on the spray plume angle has been used as boundary conditions for the simulation of droplet trajectories by injecting water droplets in the settling chamber by each spray nozzle, considering in the simulation the portion of the spray bar system reported in yellow rectangle of the *Figure 5*. *Figure 6* shows the two phases of the simulation with an indication of typical results achievable for different spray nozzle grids on the spray bar array selected for this study.

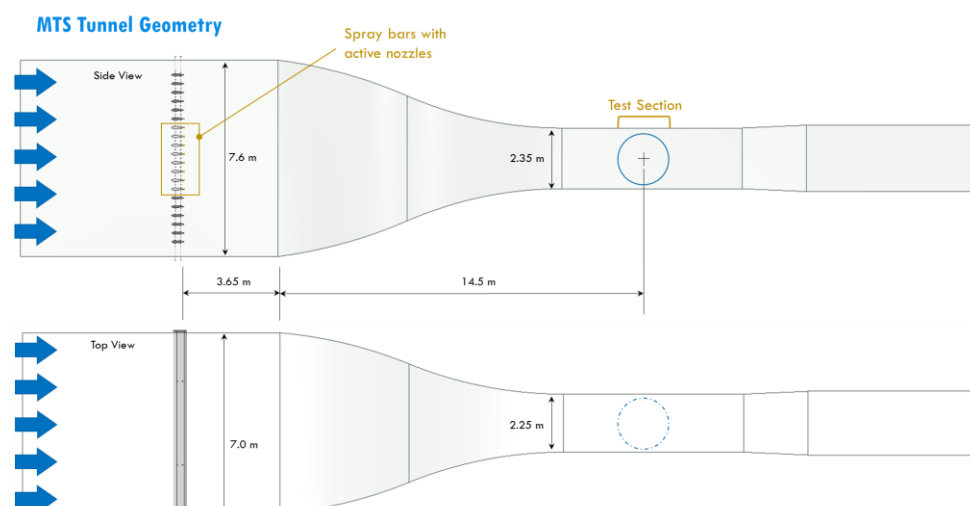


Figure 5: CIRA-IWT sketch showing the geometry considered for the CFD simulation with the test leg of the MTS configuration and the SBS.

The model predicts how far specific condition could be by uniform distribution of the main cloud parameters in the test section, including the water droplet temperature, showing for each condition the estimated cumulative volume fraction and normalized volume distribution (Figure 6 Figure 4).

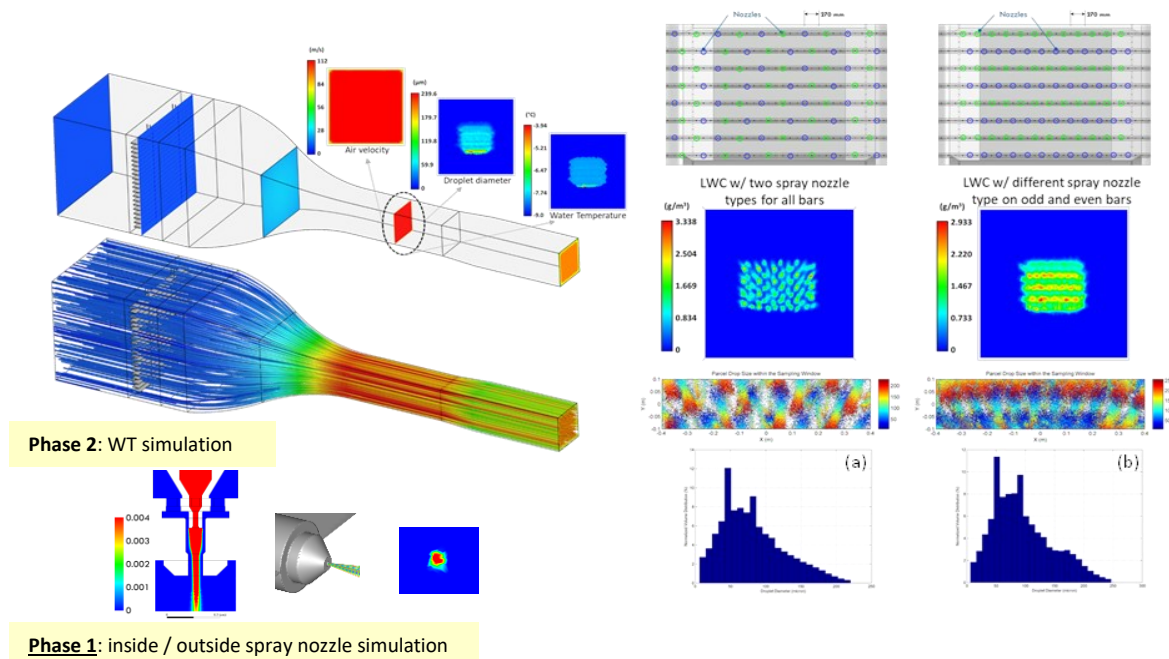


Figure 6: Study of the spray bar performance when equipped with two spray nozzle types. The first phase of this study analyses the main bi-phase flow parameters inside and outside each spray nozzle type. The simulation of the cloud inside the IWT test leg duct (phase 2) includes the assessment of LWC homogeneity with indication of potential PSD (normalized volume distribution) modifications due to different spray nozzle patterns on the spray bar module: (a) The two type of the spray nozzles are alternating on each bar; (b) each bar has a different spray nozzle (the even bars are those that produce large drops, and the odd bars are those that produce the smaller drops).

Results showing how may change the LWC distribution in the test section based on different SBS configuration and the estimated water droplet temperature achieved based on airflow conditions (droplet residence time). The example in Figure 6, shows the parcel drop size within the sampling window of the SBS for the mono-modal PSD (Figure 6a) at 0.7 gm^{-3} of LWC, and $180 \text{ }\mu\text{m}$ of MVD. This condition changing when the odd bars of the SBS are limited to injects the smaller droplets of the PSD and the even bar the large one is set to generate the bi-modal clouds resulting in higher value of LWC achieving 1.17 gm^{-1} with $134 \text{ }\mu\text{m}$ of MVD. These comparisons have been done at 110 ms^{-1} .

5.2 SBS Configurations and Rationale for the Matrix of Cloud Conditions

The SLD cloud generation has been characterized using different Spray Bar System (SBS) configurations equipped with a different density of active spray nozzles that range from 130 to 195 in function of the target values of LWC and cloud uniformity to achieve in the tests section. The SLD improvement was achieved for CIRA-IWT, selecting a new water atomizer for better cloud uniformity and coverage area in the test section for the lower LWC values than the previous SBS configuration equipped with the spray nozzle with a single jet. The new atomizer operates with multi-jet spray to increase the spray plume angle to cover a larger cross section of the spray bar when the low LWC value to target requests a reduced number of active spray nozzles. To generate the Appendix O clouds limited to the FZDZ conditions with MVD below or higher than $40 \text{ }\mu\text{m}$ and the Appendix C cloud conditions, 13 bars (from bar#4 to bar#16), each equipped with 30 spray nozzles, have been suited on the SBS for fast change

from Appendix C to Appendix O. The total of 390 spray nozzles was symmetrically distributed in the cross-section of the settling chamber to limit the effect on the cloud uniformity passing from Appendix O to Appendix C (*gravitational effects on large droplet trajectories*). The two types of spray nozzles have been alternatively installed in each spray bar (from spray bar position 11 to spray position 40), allowing the change of the SBS configuration through the remote activation of the solenoid valve in each spray nozzle to turn the water flow in or off for each one. The *Table 2: Spray bar system configurations with the indication of the type and number of active spray nozzles in use during the PSD/MVD and LWC measurements at the center of the test section*, below reports the description of the SBS configuration in use with the number of active spray nozzles, the spray nozzle type, and the number of conditions tested for each SBS configuration. The first column provides a code name for each spray bar configuration used in the matrix of conditions. The objective was to explore the full potentiality of the SBS equipped with the new nozzle type in combination with the available single-jet spray nozzle to produce a bimodal spray at low LWCs.

ID_SBS configuration	Single-jet SN # of active spray	Multi-jet SN # of active spray	Even bars # of active spray	Odd bars # of active spray	PSD / MVD meas. points (#)	LWC meas. points (#)
1A2_SLD2	195	0	105	90	38	102
1A2_SLD3	0	195	105	90	10	8
1A2_SLD5	90	105	105	90	28	47
1A3_SLD6	65	65	5	5	13	9

Table 2: Spray bar system configurations with the indication of the type and number of active spray nozzles in use during the PSD/MVD and LWC measurements at the center of the test section.

The first spray bar configuration (1A2_SLD2) has been more characterized in terms of LWC and PSD/MVD for two airspeeds (60 and 110 m/s), three pressure altitudes (0m, 1524m, and 6096m), and three SAT (-8C, -18C, -25C). This configuration represents the first baseline, able to generate Appendix C at low LWC values, contributing to the first PSD mode in the bi-modal FZDZ clouds. The second baseline is the SBS configuration 1A2_SLD3 with only multi-jet spray nozzles active. This configuration can inject droplets within the wide-angle spray plume, producing a large spatial distribution with low water droplet concentration for the single-jet spray nozzle. *Figure 7* shows an example of a comparison between the two spray nozzles at the same air/water pressure settings using a Laser Sheet Imaging (LSI) method to measure the intensity of the spray plume showing different spray concentration distribution in terms of size, shape and relative distribution of the spray plume at the same distance from the nozzle exit. Measurements were performed by Spraying Systems & Co. in ambient conditions using their open circuit aerodynamic wind tunnel by installing the in the test section spray nozzle to study the spray plume characteristics when submitted at the same airspeed of the CIRA-IWT settling chamber (10 ms⁻¹).

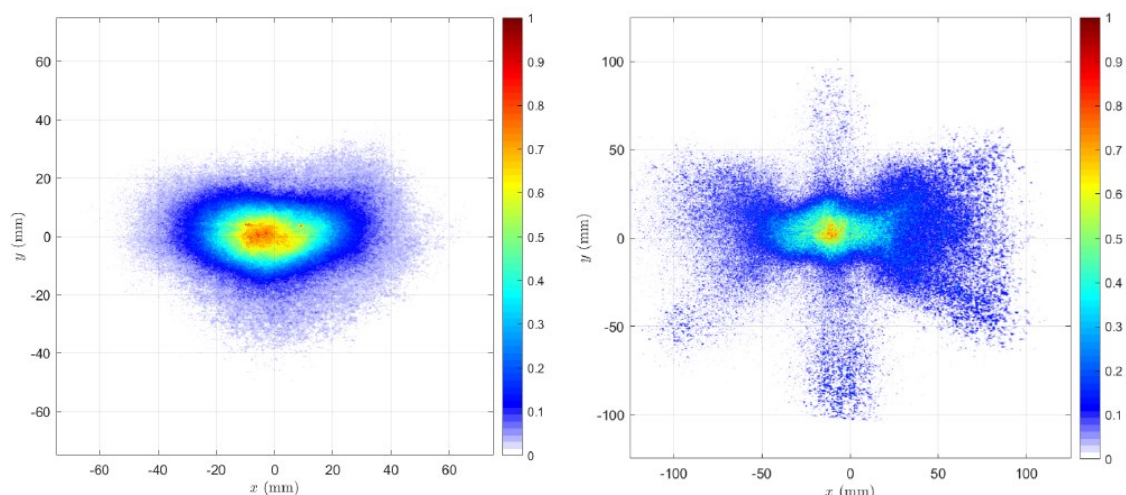


Figure 7: Water spray concentration measured by LSI system in the spray plume generated by single-jet (on the left) and multi-jet (on the right) spray nozzle.

The last two SBS configurations shown in Table 2, 1A2_SLD5 and 1A2_SLD6, have been tested to measure the potential capability to generate the bi-modal PSD. For the first one, the air and water pressure settings of the even bars were chosen to produce large droplets, while the pressure settings of the odd bars were chosen to produce small droplets. In this configuration, the capability to modulate the mass flow, whether for a small or large size range, determines the degree of variability of the small and large modes in the bi-modal PSD. The last SBS configuration, 1A3_SLD6, has been used by setting all the bars at the same water and air pressures and using different spray nozzle features to generate small and large particles from the same bar. The total number of spray nozzles has been reduced for this configuration to allow the generation of clouds at lower LWC.

The following sections describe the measurement executed for each configuration of the SBS and the results obtained with this first part of CIRA-IWT cloud characterization.

5.3 PSD/MVD Measurements and Preliminary Results for FZDZ Conditions

The measurements activities in the CIRA-IWT were planned to a single slot from April 2022 to early June 2022 with the objective to collect enough data to support WP8 test campaign, just after the calibration activities. For this reason, not enough condition points were measured to collect a valid number of statistical data to determine general calibration curves for MVD/PSD to correlate with LWCs data.

5.3.1 PSD/MVD Test Matrix

The test matrix has been defined considering the cloud conditions based on past air and water pressure settings already tested in CIRA-IWT with the single-jet spray nozzle. For the airflow, the conditions were based on the requirements foreseen for the WP8 test campaign to be performed just after the end of the measurements of CIRA-IWT cloud calibration. For this reason, the flow conditions were defined for two airspeeds and three pressure altitudes. The matrix below (Table 3) reports all the airflow and SBS settings used during the measurements with DLR CCP probe from May 3rd to May 5th, 2022.

Cloud Co	V	Ts	Ttot	h	Pairever	Pwateve	Pairodd	Pwatodd	GRID-Nozzle Typ
8	60	-2	-0,2	1524	50	30	50	30	1A2_SLD#2
8	60	-2	-0,2	6096	50	30	50	30	1A2_SLD#2
104	110	-8	-2	6096	221	166	221	166	1A2_SLD#2
97	110	-8	-2	6096	220	164	220	164	1A2_SLD#2
105	110	-8	-2	6096	107	81	107	81	1A2_SLD#2
53	110	-8	-2	6096	110	60	110	60	1A2_SLD#2
96	110	-8	-2	6096	123	67	123	67	1A2_SLD#2
27	110	-8	-2	6096	60	40	60	40	1A2_SLD#2
9	100	-6	-1	0	20	20	20	20	1A2_SLD#2
10	110	-6	0	0	30	20	30	20	1A2_SLD#2
30	110	-6	0	0	70	40	70	40	1A2_SLD#2
96	60	-2	-0,2	1524	123	67	123	67	1A2_SLD#2
53	60	-2	-0,2	1524	110	60	110	60	1A2_SLD#2
26	60	-2	-0,2	1524	60	30	60	30	1A2_SLD#2
7	60	-2	-0,2	1524	20	10	20	10	1A2_SLD#2
25	60	-2	-0,2	6096	60	20	60	20	1A2_SLD#2
26	60	-2	-0,2	6096	60	30	60	30	1A2_SLD#2
27	60	-2	-0,2	6096	60	40	60	40	1A2_SLD#2
9	60	-2	-0,2	6096	20	20	20	20	1A2_SLD#2
96	60	-2	-0,2	6096	123	67	123	67	1A2_SLD#2
97	60	-2	-0,2	6096	220	164	220	164	1A2_SLD#2
99	110	-6	0	1524	301	207	301	207	1A2_SLD#2
97	110	-6	0	1524	220	164	220	164	1A2_SLD#2
100	110	-6	0	1524	129	86	129	86	1A2_SLD#2
96	110	-6	0	1524	123	67	123	67	1A2_SLD#2
53	110	-6	0	1524	110	60	110	60	1A2_SLD#2
98	110	-6	0	1524	123	50	123	50	1A2_SLD#2
26	110	-6	0	6096	60	30	60	30	1A2_SLD#2
25	110	-6	0	6096	60	20	60	20	1A2_SLD#2
9	110	-6	0	6096	20	20	20	20	1A2_SLD#2
26	110	-6	0	1524	60	30	60	30	1A2_SLD#2
41	110	-6	0	1524	70	50	70	50	1A2_SLD#2

IC

Cloud Co	V	Ts	Ttot	h	Pairever	Pwateve	Pairodd	Pwatodc	GRID-Nozzle Typ
75	110	-6	0	6096	20	10	20	10	1A2_SLD#3
73	110	-6	0	6096	60	30	60	30	1A2_SLD#3
72	110	-6	0	6096	30	20	30	20	1A2_SLD#3
71	110	-6	0	0	70	40	70	40	1A2_SLD#3
72	110	-6	0	0	30	20	30	20	1A2_SLD#3
75	110	-6	0	0	20	10	20	10	1A2_SLD#3
76	110	-6	0	0	20	20	20	20	1A2_SLD#3
78	110	-6	0	0	70	20	70	20	1A2_SLD#3
73	110	-6	0	0	60	30	60	30	1A2_SLD#3
88	110	-6	0	0	50	30	50	30	1A2_SLD#3
87	60	-2	-0,2	1524	70	40	190	100	1A2_SLD#5
86	60	-2	-0,2	1524	60	30	190	100	1A2_SLD#5
85	60	-2	-0,2	1524	50	40	190	100	1A2_SLD#5
84	60	-2	-0,2	1524	40	20	190	100	1A2_SLD#5
83	60	-2	-0,2	1524	50	20	190	100	1A2_SLD#5
110	60	-2	-0,2	1524	20	30	190	100	1A2_SLD#5
83	60	-2	-0,2	6096	50	20	190	100	1A2_SLD#5
84	60	-2	-0,2	6096	40	20	190	100	1A2_SLD#5
85	60	-2	-0,2	6096	50	40	190	100	1A2_SLD#5
86	60	-2	-0,2	6096	60	30	190	100	1A2_SLD#5
87	60	-2	-0,2	6096	70	40	190	100	1A2_SLD#5
110	60	-2	-0,2	6096	20	30	190	100	1A2_SLD#5
127	110	-6	0	6096	20	30	301	207	1A2_SLD#5
85	110	-6	0	6096	50	40	190	100	1A2_SLD#5
86	110	-6	0	6096	60	30	190	100	1A2_SLD#5
87	110	-6	0	6096	70	40	190	100	1A2_SLD#5
85	110	-6	0	1524	50	40	190	100	1A2_SLD#5
87	110	-6	0	1524	70	40	190	100	1A2_SLD#5
128	110	-6	0	1524	40	30	190	100	1A2_SLD#5
127	110	-6	0	1524	20	30	301	207	1A2_SLD#5
110	110	-6	0	1524	20	30	190	100	1A2_SLD#5
111	110	-6	0	1524	20	20	190	100	1A2_SLD#5
86	110	-6	0	1524	60	30	190	100	1A2_SLD#5
81	110	-6	0	0	20	20	20	20	1A3_SLD#6
82	110	-6	0	0	20	40	20	40	1A3_SLD#6
83	110	-6	0	0	50	20	190	100	1A2_SLD#5
84	110	-6	0	0	40	20	190	100	1A2_SLD#5
85	110	-6	0	0	50	40	190	100	1A2_SLD#5
86	110	-6	0	0	60	30	190	100	1A2_SLD#5
87	110	-6	0	0	70	40	190	100	1A2_SLD#5
80	110	-6	0	0	40	50	40	50	1A3_SLD#6
115	110	-6	0	0	30	20	30	20	1A3_SLD#6
116	110	-6	0	0	30	30	30	30	1A3_SLD#6
117	110	-6	0	0	30	90	30	90	1A3_SLD#6
118	110	-6	0	0	40	20	40	20	1A3_SLD#6
119	110	-6	0	0	40	30	40	30	1A3_SLD#6
120	110	-6	0	0	50	20	50	20	1A3_SLD#6
121	110	-6	0	0	50	30	50	30	1A3_SLD#6
123	110	-6	0	0	50	40	50	40	1A3_SLD#6
124	110	-6	0	0	60	30	60	30	1A3_SLD#6
125	110	-6	0	0	60	40	60	40	1A3_SLD#6

Table 3: Matrix of cloud conditions (in the first column) used during the PSD/MVD cloud characterization with DLR CCP probe.

5.3.2 PSD/MVD Results from Preliminary SLD Calibration

The assessment of the FZDZ conditions in CIRA-IWT were mainly supported by DLR using the CCP probe (Figure 8), which is a combination of scattering technique, CDP with a $2 \mu\text{m} - 50 \mu\text{m}$ size range, and CIP-G probe, an Optical Array Probe with a $15 \mu\text{m} - 930 \mu\text{m}$ size range. CIRA 4D-PDI probe with size range $1 \mu\text{m} - 698 \mu\text{m}$ has also been used during the measurements for low concentration cloud conditions.



Figure 8: DLR CCP (Cloud Combination Probe) on the left, installed in the centerline of the CIRA IWT test section during the PSD/MVD measurement slot. CIRA 4D-PDI on the right installed with sample volume located on the centerline, in the same position of DLR CCP.

The measurements have been performed at the centre of rotation of the model support system after cloud uniformity check performed with icing cylinders.

In Figure 9, the resulting PSDs are compared with the reference cumulative volume fraction described in Appendix O. Cloud conditions are generated using the single-jet spray nozzle with the spray bar configuration 1A2_SLD2.

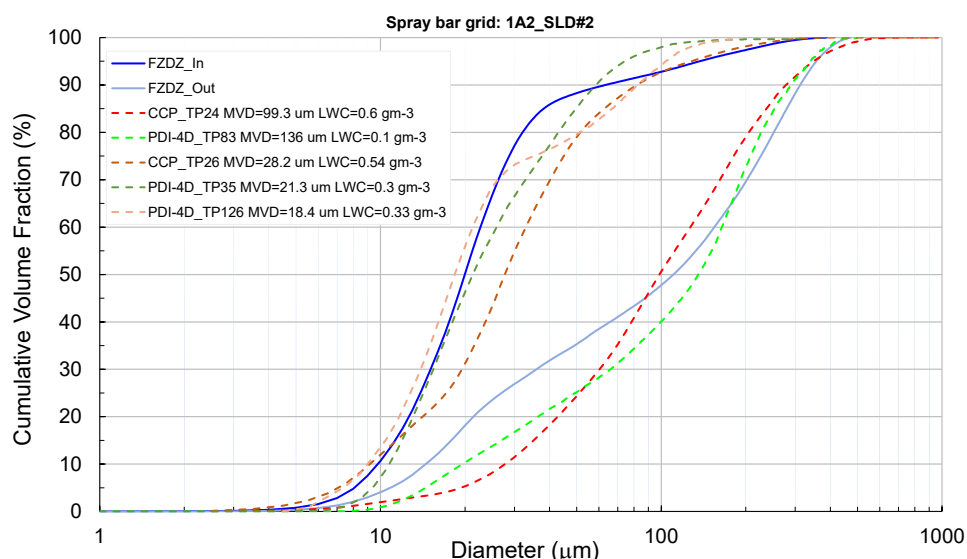


Figure 9: Cumulative volume fraction measured for each test point (TP) by CCP and 4D-PDI at 110 ms^{-1} , with 1A2_SLD2 of SBS configuration.

The three dashed curves collected by CCP and PDI-4D show some variability to agree with the full reference curve of FZDZ below the $40 \mu\text{m}$ from about 70% of cumulative volume fraction, even if the two 4D-PDI measurements are quite close below this value. For the cloud generated with this spray

bar configuration, the data measured showed the MVD changes between 18.4 μm and 21.3 μm and LWC ranging from 0.3 to 0.54 gm-3.

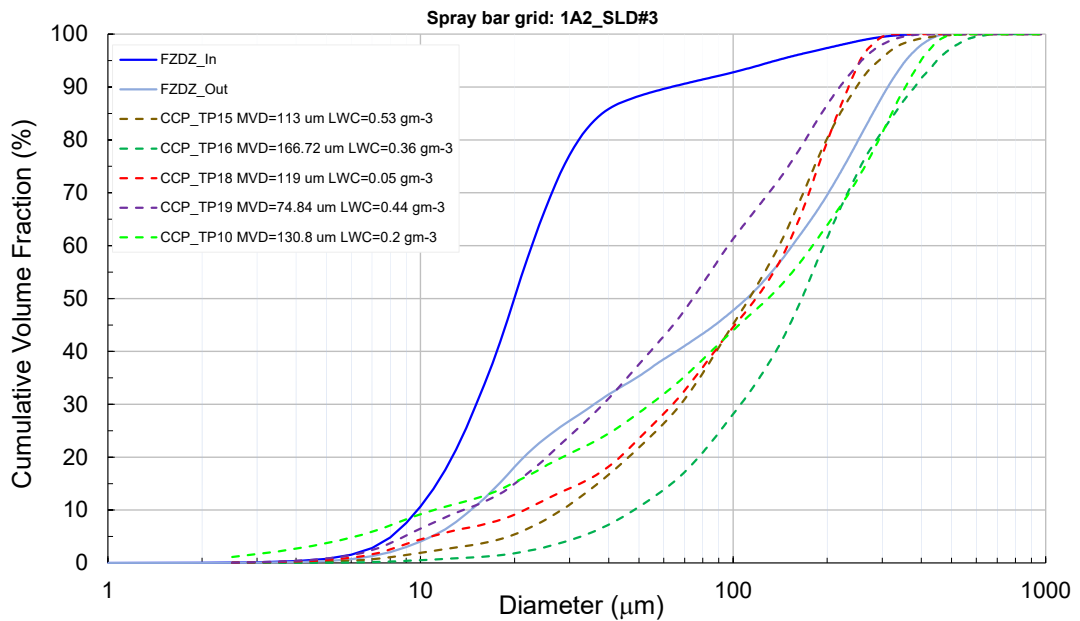


Figure 10: Cumulative volume fraction measured by CCP probe at 110 ms-1 measured with 1A2_SLD3 of SBS configuration.

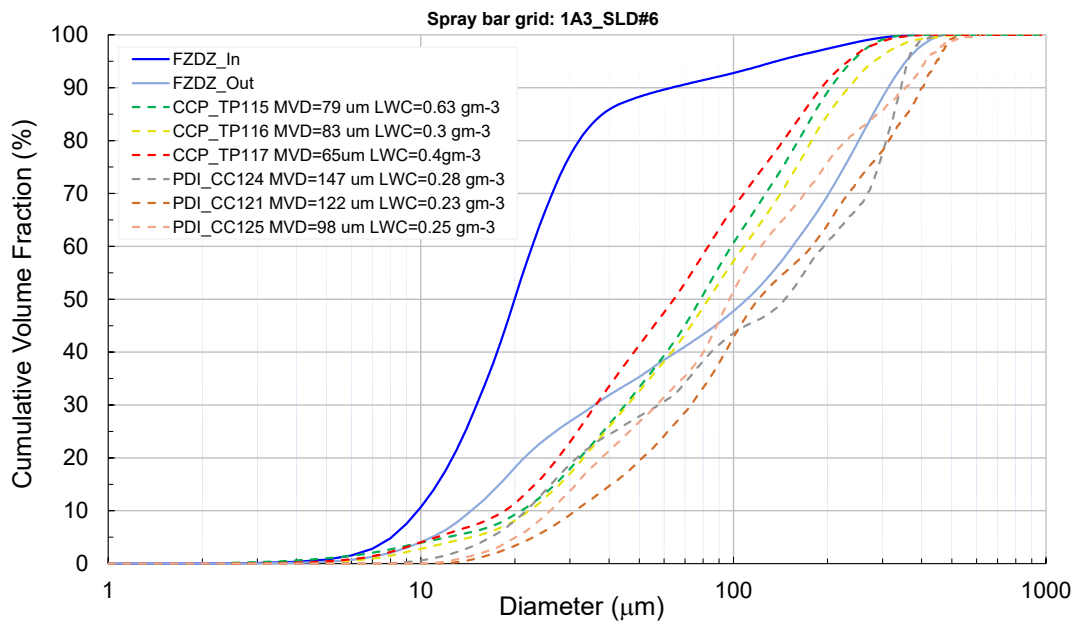


Figure 11: Cumulative volume fraction measured by CCP and PDI probe at 110 ms-1 measured with 1A3_SLD6 of SBS configuration.

Figure 9 to Figure 12 shows the features of each spray bar configuration to generate clouds for some conditions close to the FZDZ cumulative volume fractions curves for MVD below and higher than 40 μm at low liquid water content values. Some other conditions are far from target PSD requirement and this is manifested by the fact of data processing and analysis has not been followed by a second measurement slot with adjusted air/water pressure settings. What has been learned from these first results is how the influence of the SBS configurations (spray nozzle types ratio) is sensitive to the facility's target requirements (Appendix O).

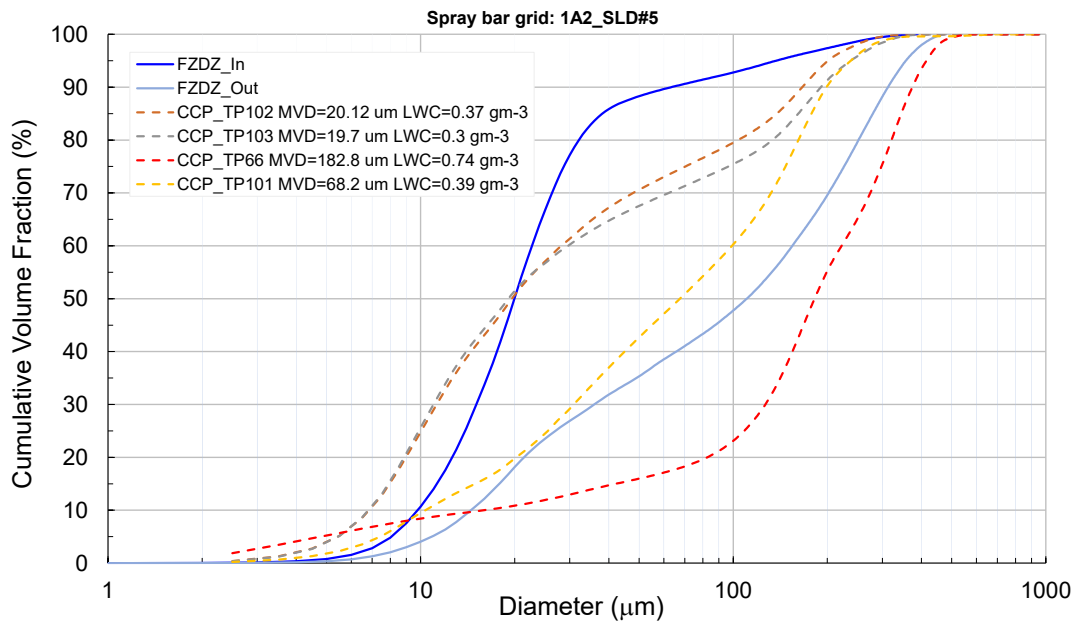


Figure 12: Cumulative volume fraction measured by CCP and PDI probe at 110 ms⁻¹ measured with 1A2_SLD5 of SBS configuration.

In particular, the SBS with 1A2_SLD2 grid configuration equipped with single-jet spray nozzles allows the generation of low MVD at low LWC and provides most of the monomodal PSDs for both FZDZ envelopes. This configuration will be consistent with the values to achieve with FZDZ with MVD < 40 µm (**FZDZ-In**). Considering the same number of active sprays, 195, using the multi-jet spray nozzles with 1A2_SLD3 spray bar grid configuration, the PSD shape becomes, for most of the conditions tested, bi-modal and close to the target PSDs for some conditions, as shown for the case of the test point 10 reported in Figure 10 as an example.

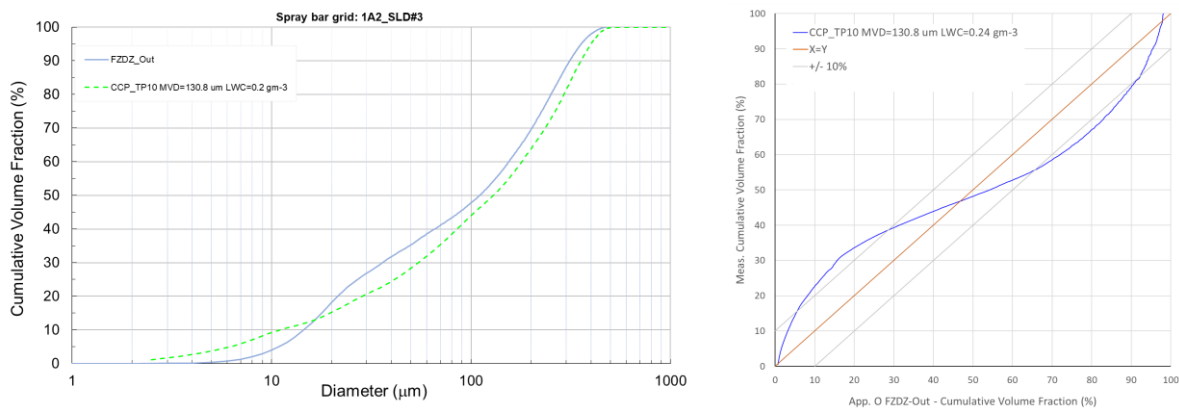


Figure 13: Example of the quantile-quantile plot showing the agreement between the measured PSD and Appendix O requirement with 1A2_SLD3 spray bar configuration. Data has been collected by CCP probe at 110 ms⁻¹ and at pressure altitude of 6096 m.

To quantify the degree of agreement between reference PSD in Appendix O and test point 10, Figure 13 reports the quantile-quantile plot showing how their difference changes for the full diameter range within the uncertainty threshold determined by the PSD target requirement. For this cloud condition, the deviation from the reference PSD is almost outside by 10%, even if must be highlighted that small changes in the spray bar settings may influence the behaviour shown in Figure 13.

The SBS with 1A2_SLD3 grid configuration shows an advantage in changing the PSD shapes from mono-modal to bi-modal for the FZDZ with MVD>40µm (**FZDZ-Out**). This configuration has limitations in generating the small droplets and, thus, difficulties in covering the envelope defined in the FZDZ-In. Despite the advantage of overlapping the FZDZ-Out, this SBS configuration shows some difficulties in

maintaining the requested bi-modal PSD shape by changing the mass concentration for each of the two modes of PSD of FZDZ-Out requirement through the variation of the spray bar pressure settings, keeping the LWC within the target values ($< 0.3 \text{ gm}^{-3}$) for expected airspeed range (e.g., from 60 ms^{-1} to 120 ms^{-1}). At this end, the use of SBS with 1A3_SLD6 and the 1A2_SLD5 grid configurations (*Figure 11* and *Figure 12*) are able to produce bi-modal PSDs at low LWC respectively with a medium and high level of controllability of small and large mode of the PSDs shapes.

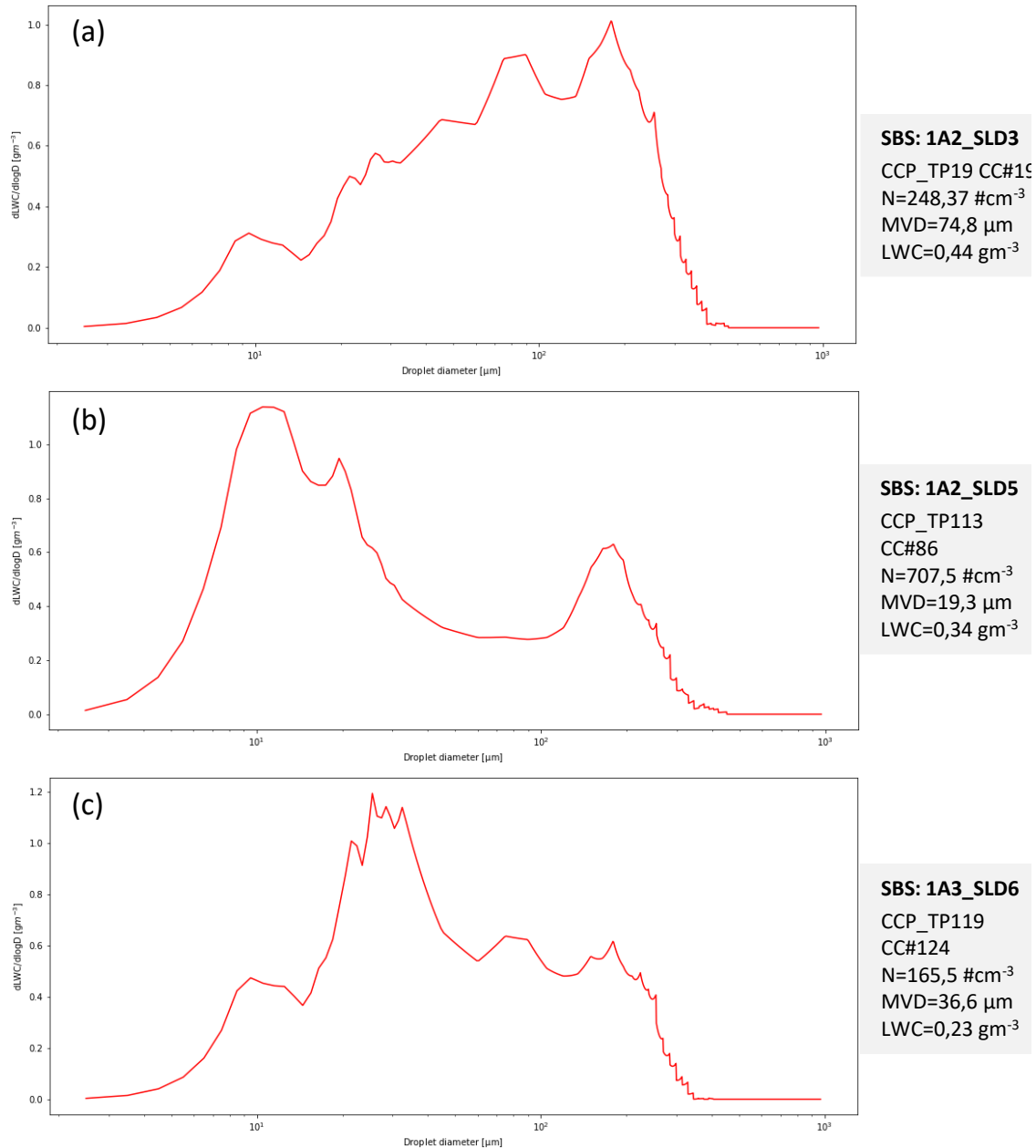


Figure 14: Effect of the spray bar configurations on water mass distribution for the same condition: 110 ms^{-1} of airspeed with the SBS setting at the same air and water pressures (case a and c) excluding the case (b) with half spray nozzles setting at higher pressures to generate the smaller droplets.

An example of variability in the PSD shape is provided by Figure 14, which shows the sensitivity of the CIRA-IWT spray bar system with the $dLWC/dlogD$ plots. The area below these plots represents the LWC of the artificial clouds generated with the air pressure at 60 kPa and the water pressure at 30 kPa for each spray bar configuration shown in this figure excluding the case of *Figure 6 b*, where only the even bars (105 multi-jet spray nozzles, see *Table 2*) are setting to the same air and water pressures to contribute for large droplets concentration in the cloud. Thus, the 1A2_SLD5 spray bar configuration has the same number (195) of active spray nozzles as the 1A2_SLD3, but almost half of active spray

nozzles (90 with the single jet type) contribute to the concentration for the lower part of PSD diameter represented in the *Figure 14 b*. Therefore, by changing the air and water pressures only for the odd bars, the concentration of the small droplet diameter range in the PSD mode in *Figure 14 b* can be modified. PSD/MVD cloud calibration for FZDZ with such spray bar configuration requests an iterative measurement process that includes attempt data processing and analysis followed by an additional measurement section to finalize the full calibration at different flow conditions (airspeed and pressure altitude).

5.4 LWC measurements

Measurements have been performed at the centre of rotation of the model support system with SEA WCM-2000 with multi-wire (MW) by using its total water content (TWC) sensing element and the Robust Probe (RP). The second hot-wire sensor agrees well with the MW and provides a more accurate measurement for larger MVD ($> 200 \mu\text{m}$) for assessing if some SBS settings are providing unexpected FZRA clouds [8]. *Figure 15* shows the set-up of the RP during the measurement section. Up to 150 test points were collected during the measurements, most with the 1A2_SLD2 spray bar configuration to characterize the full LWC envelope at 110 ms^{-1} and sea level pressure altitude. The LWC for the other SBS configurations has been characterized only for some limited conditions for checking achievable LWC values.

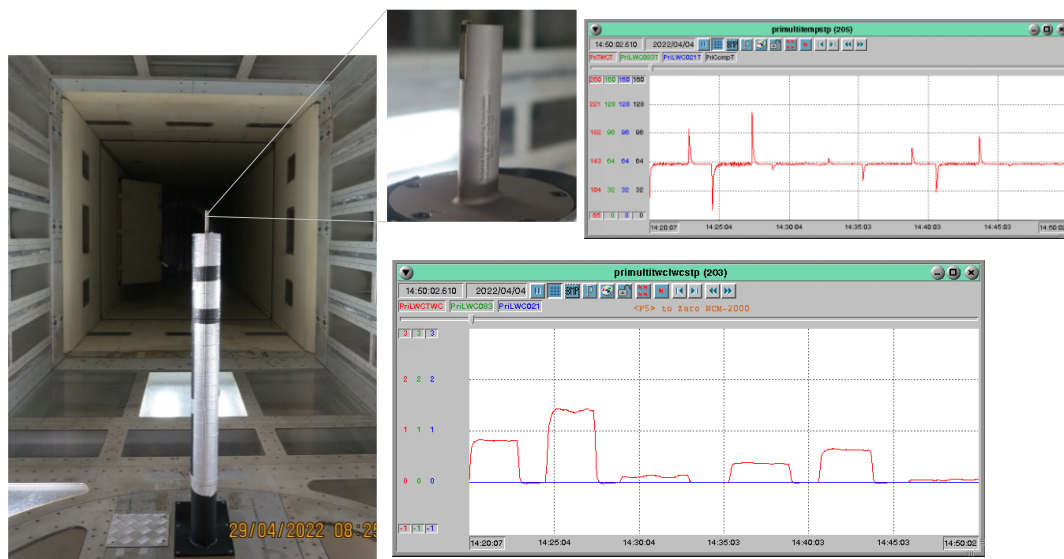


Figure 15: LWC measurements with RP installed on the strut to locate its sampling volume at the centerline of the CIRA-IWT test section. The plot on the top shows the sensor element temperature during the acquisition and between each test point. TWC behaviour for some conditions is shown in the bottom plot.

The collision efficiency is an important correction factor for hot-wire probes and has been determined on the base of sensing element geometry in agreement to the reference [8]. This parameter describes the impingement of water droplets due to their inertia, drag, and interaction with the aerodynamic flow field and do not include splashing and re-entrainment of droplets impacting the sensor, which can dominate net sensor efficiency especially for SLD. For each test point, an appropriate time average of the measurements to show stable values (e.g., 60, 90, or 120 seconds) have been collected at total air temperature below zero to prevent droplets re-circulation. The dry power response has been directly extracted by the sensing element taking a stable dry period when spray is not present. Between each spray point, the dry power value has been verified with $\text{LWC}=0 \text{ g m}^{-3}$ to ensure that neither droplet re-circulation nor ice formation on the sensing element or around the probe that may affect the accuracy of subsequent measurement points would occur.

For available measurement slot, only one SBS configuration, the 1A2_SLD2, have been characterized and results are shown in *Figure 16*.

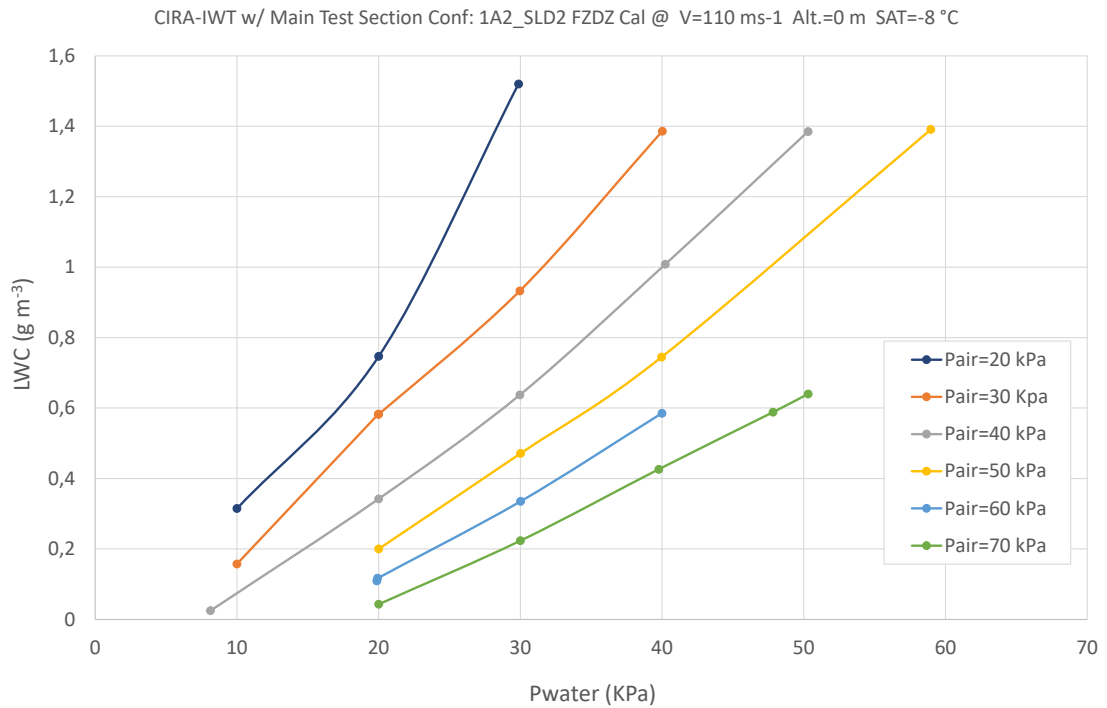


Figure 16: Cloud LWC calibration generated by 1A2_SLD2 spray bar configuration at 110 ms⁻¹ and with pressure altitude at sea level.

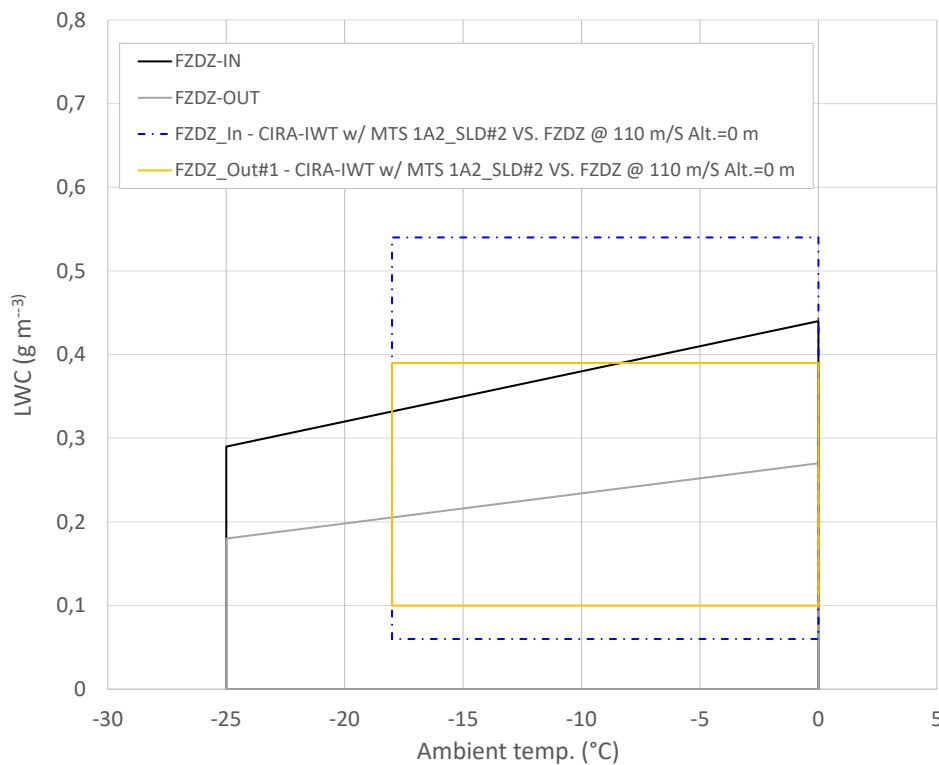


Figure 17: LWC calibration envelope for FZDZ cloud conditions generated by 1A2_SLD2 spray bar configuration

Data have been collected at -8 °C of air temperature, but the same conditions have been tested up to -18 °C. Figure 17 above compares the envelope covered by the same SBS configuration over a range of SAT with the FZDZ requirement. Further measurements with other SBS configurations must be performed considering the wide potentiality of improvement of the SLD cloud envelope in CIRA-IWT.

5.4.1 LWC uniformity

Preliminary assessment of cloud uniformity and coverage area in the reference plane at the centre of rotation of the model support system has been performed for each spray bar configuration at low, 60 ms^{-1} , and high speed, 110 ms^{-1} .



Test #04

$V = 60 \text{ m/s}$, $T = -10^\circ\text{C}$, $h = \text{s.l.}$, $P_a = 60 \text{ kPa}$, $P_w = 30 \text{ kPa}$
grid=1A2_SLD#3 - MVD = 40 μm LWC = 0,5 gm^{-3}

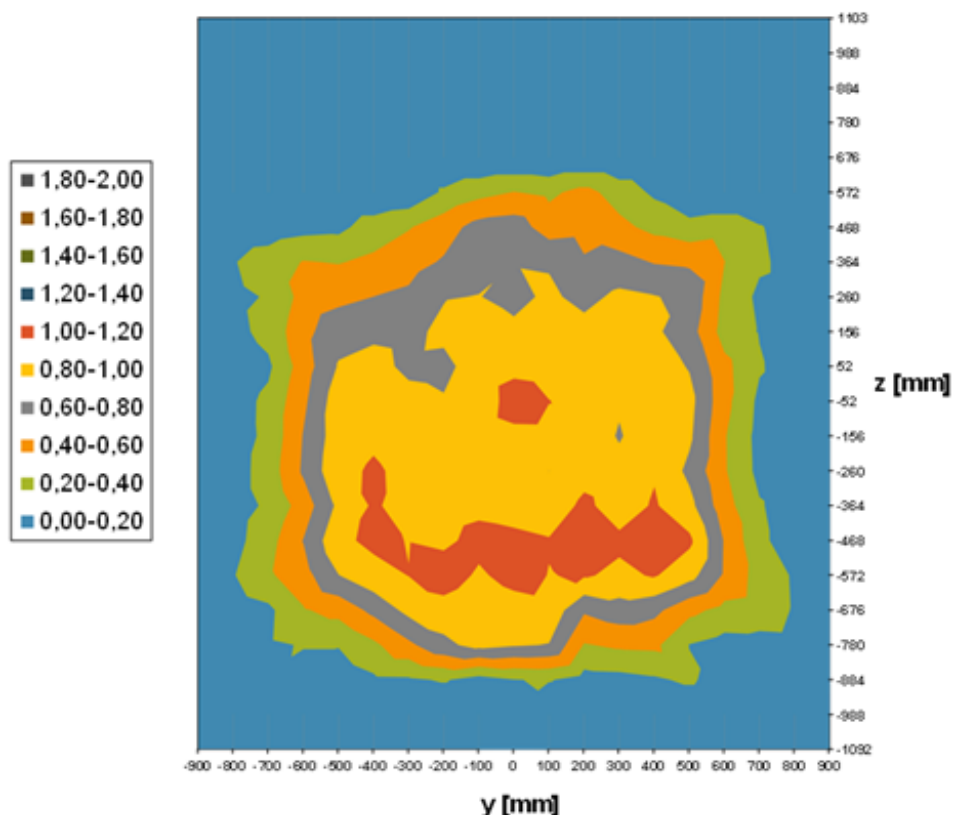


Figure 18: Cloud uniformity for one of the Appendix C conditions was measured with an Icing Grid at 60 ms^{-1} at sea level of pressure altitude. Cloud has been generated with 1A2_SLD3 spray bar configuration at minimum MVD.

For this task, both the Icing Calibration Grid (IG) and the Icing Cylinders (IC) method have been used. The first method mainly applied for the Appendix C, according to the guidelines of ARP 5905 (Aerospace Recommended Practice SAE ARP5905, Sept. 2015). At low MVDs, the IG will provide quantitative information on the local LWC and thus its spatial distribution through contour maps derived by using a dimensionless ratio of the LWC at a given location in the test section divided by the LWC at the centre of the test section. The LWCs are derived from ice thickness measurements at midpoints of vertical IG components. For the measured test cases, a good coverage and cloud uniformity in reference area have been found with expected LWC variation within $\pm 20\%$ as shown the example reported in *Figure 18*. *Figure 19* shows an example of the result achieved by cloud uniformity check for a typical Appendix O conditions with the ice thickness along the IC collected at 110 ms^{-1} for $110 \mu\text{m}$ of MVD and 0.5 gm^{-3} of LWC. The plot in *Figure 19* highlights how the ice thickness values on the three cylinders, normalized to the center value of the central cylinder, fall within the threshold limits of $\pm 20\%$.

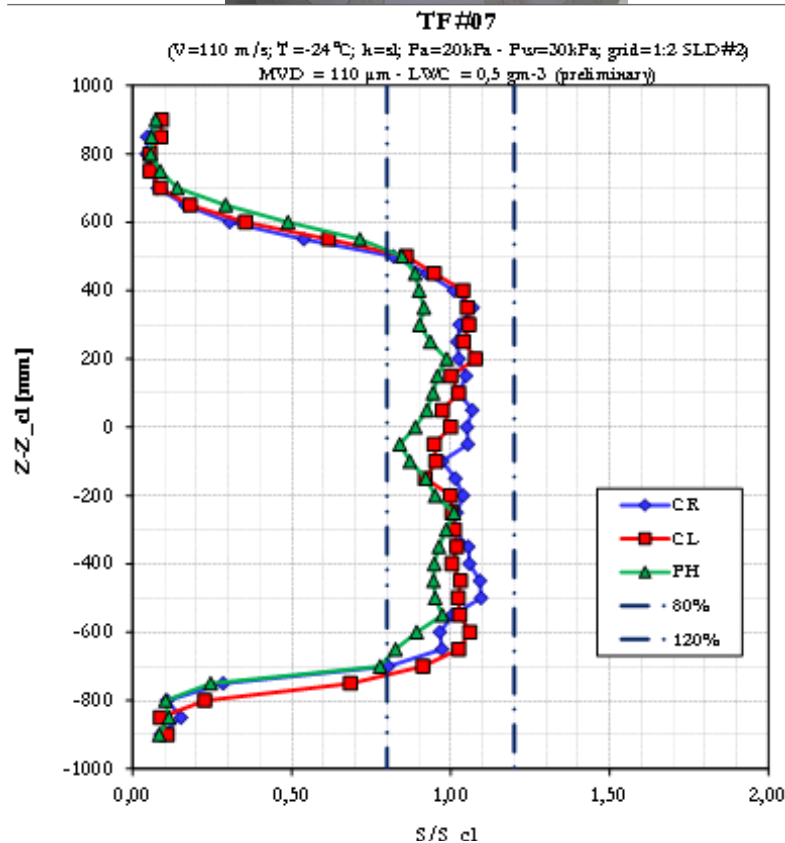


Figure 19: Variation of the ice thickness along the three cylinders located in the reference area of the test section. 1A2_SLD2 spray bar configuration has been used to generate 110 μm of MVD cloud with 0.5 gm^{-3} of LWC.

6 Conclusion

The selection of a new spray nozzle setup using a retrofit of the current SLD spray nozzle adds great flexibility in generating clouds at low LWC and controllable bi-modal PSDs, specifically adopting different air and water pressures for odd and even bars.

A full calibration of CIRA-IWT is expected to complete the Appendix O envelopes using the validated calibration methodology defined in the reference [9] to better identify the achievement of facilities target requirements for Appendix O [10]. This process will pass through the completion of the measurements for all possible sets of SBS configurations in which cloud conditions fall within the Appendix O envelopes at low and high airspeed with the possibility to change the pressure altitude. Considering the complexity of the calibration activity, CIRA will finalize with SEA, Met Analytics Inc., NCAR, and NASA's new PSD measurement method 1D2D-X [11], which will allow to show the real-time 1D spectrum with the possibility of more advanced real-time particle rejection and processing using algorithms to provide a droplet spectrum with adequate comparability to more sophisticated post-processing. The goal is to produce a simple 1D PSD data stream in real-time during the measurements that will allow estimation of PSD shape and adequately identify bi-modality requested by Appendix O. The intent is to optimize and make more efficient CIRA-IWT calibration for Appendix O.

7 References

- [1] European Union Aviation Safety Agency (EASA), "Certification Specifications and Acceptable Means of Compliance for Large Aeroplanes (CS-25) Amendment 27," 2021.
- [2] S. G. Cober, A. D. Isaac, A. D. Shah und R. Jeck, „Characterizations of aircraft icing environments that include supercooled large drops," *J. Appl. Meteor.*, Bd. 40, pp. 194-2002, 2001.
- [3] G. A. Isaac, S. G. Cober, W. Strapp, A. V. Korolev, A. Trembler und D. L. Marcotte, „Recent Canadian research on aircraft in-flight icing," *Can. Aeronaut. Space J.*, Bd. 47, pp. 213-221, 2001.
- [4] A. J. Curry, „FIRE Arctic Clouds Experiment," *Bull. Amer. Meteor. Soc.*, Bd. 81, pp. 5-29, 2000.
- [5] G. A. Isaac, S. G. Cober, J. W. Strapp, D. Hudak, T. P. Ratvasky, D. L. Marcotte und F. Fabry, „Preliminary Results from the Alliance Icing Research Study (AIRS)," *39th AIAA Aerospace Science Meeting and Exhibit*, p. 12 pp, 2001.
- [6] D. Miller, T. Ratvasky, B. Bernstein, F. McDonough and J. W. Strapp, "NASA/FAA/NCAR supercooled large droplet icing flight research," *American Institute of Aeronautics and Astronautics*, no. AIAA 98-0577, p. 24pp, 1998.
- [7] S. G. Cober and I. A. George, "Characterization of Aircraft Icing Environments with Supercooled Large Drops for Application to Commercial Aircraft Certification," *Journal of Applied Meteorology and Climatology*, no. Volume 51, pp. 265-284, 2012.
- [8] Federal Aviation Administration FAA, "Data and Analysis for the Development of an Engineering Standard for Supercooled Large Drop Conditions," DOT/FAA/AR-09/10, National Technical Information Services (NTIS), Springfield, Virginia 22161, 2009.
- [9] Ice-GENESIS Public Deliberable D6.1-D6.2: Proposal of Calibration Instruments and Procedures for FZDZ and FZRA
- [10] Ice-GENESIS Public Deliberable D3.1: Definition of the target requirements for test facilities operating envelopes for App O," 2024
- [11] Lilie, L., Bouley, D., Sivo, C., Esposito, B. et al., "A New 1D2D Optical Array Particle Imaging Probe for Airborne and Ground Simulation Cloud Measurements," SAE Technical Paper 2023-01-1415, 2023, doi:10.4271/2023-01-1415.